Speckle Noise Reduction in SAR Imagery Using a Local Adaptive Median Filter

Fang Qiu
Program in Geographic Information Sciences, University of Texas at Dallas, Richardson, Texas 75083-0688

Judith Berglund,[1] John R. Jensen
Department of Geography, University of South Carolina, Columbia, South Carolina 29208

Pathik Thakkar, and Dianwei Ren
Program in Geographic Information Sciences, University of Texas at Dallas, Richardson, Texas 75083-0688

Abstract: Speckle noise is the grainy salt-and-pepper pattern present in radar imagery caused by the interaction of out-of-phase waves with a target. A local adaptive median filter was developed that uses local statistics to detect SAR speckle noise and to replace it with a local median value. The performance of the local adaptive median filter was evaluated using RADARSAT and JERS-1 datasets based on both visual assessment and a number of numerical measures. In comparison with established filters, it was found that the local adaptive median filter outperformed others in achieving the best balance between speckle suppression and image detail preservation.

INTRODUCTION

Synthetic-aperture radar (SAR) uses microwave radiation to illuminate the Earth's surface. An image is formed after the SAR system receives the coherent sum of reflected radiation at the antenna that is synthesized by the large motion of the sensor system. Since SAR provides its own illumination, it overcomes some of the fundamental problems associated with conventional passive remote sensing. For example, SAR is not affected by cloud cover or variation in solar illumination, and thus can operate day or night. Under certain circumstances, radar can partially penetrate arid and hyper-arid surfaces, revealing subsurface features of the Earth. Although radar does not penetrate standing water, it can reflect the surface action of

[1]Judith Berglund is now with Lockheed Martin Space Operations–Stennis Programs, NASA John C. Stennis Space Center, MS 39529-6000.

GIScience and Remote Sensing, 2004, **41**, No. 3, pp. 244-266.

oceans, lakes, and other bodies of water and may sometimes provide information about the bottom features of the water body (Jensen, 2000).

Electromagnetic waves emitted by active sensors travel in phase and interact minimally on their way to the target area. After interaction with the target, these waves are no longer in phase even though they are coherent in frequency. This is caused by several factors, such as the difference in distance the waves travel back from different targets, or the single versus multiple bounce scattering due to the variance in surface roughness. Hervet et al. (1998) also noted that when the synthesized antenna moves, the signals may go out of phase. The out-of-phase waves interfere constructively or destructively to produce stronger or weaker signals. When a SAR image is formed by coherently processing the backscatter returns from successive radar pulses, this effect causes a pixel-to-pixel variation in intensity, which manifests itself as a salt-and-pepper granular pattern called *speckle* (or fading) (Goodman, 1976; Lee et al., 1994). These bright and dark pixels result in a SAR image that fails to have a constant mean radiometric level in homogeneous areas (Bruniquel and Lopes, 1997).

Radar speckle noise has a standard deviation linearly related to the mean and is often modeled as a multiplicative process. This means that the higher the signal strength the higher the noise. As a result, more speckle noise is commonly present near brighter pixel areas (North and Wu, 2001). According to Hervet et al. (1998) and Schulze and Wu (1995), the statistics of the speckle noise are well known. The noise of single-look SAR amplitude imagery often has a Rayleigh distribution, whereas that of single-look intensity imagery has a negative exponential distribution. Multi-look SAR imagery usually follows a gamma distribution, assuming the looks are independent (Lee, 1986; April and Harvy, 1991).

The presence of speckle may decrease the utility of SAR imagery by reducing the ability to detect ground targets and obscuring the recognition of spatial patterns (Sheng and Xia, 1996). Consequently, it not only complicates visual image interpretation, but also makes automated digital image classification a difficult problem. Therefore, speckle noise in radar data must often be reduced before the data can be used for further analysis or information extraction. Dozens of despeckle filters have been proposed (e.g., Frost et al., 1981; 1982; Lee 1981, 1986; Kuan et al., 1987; Eliason and McEwen, 1990; Lopes et al., 1993) in order to remove multiplicative speckle noise. In general, no filter consistently outperforms others. Each filter has its unique strengths and limitations. Thus, the choice of which filter to use is dependent on the requirements of the specific application and the characteristics of the dataset employed (Lee et al., 1994). Despeckle filters with good noise removal capabilities often tend to degrade the spatial and radiometric resolution of an original image and cause the loss of image detail. This may be acceptable for applications involving large scale image interpretation or mapping. However, in many cases where the retention of the subtle structures of the image is important, the performance of noise suppression must be balanced with the filter's effectiveness in order to preserve fine detail (Xiao et al., 2003).

This research presents a new local adaptive median filter aimed at simultaneously suppressing speckle noise while preserving the subtle image detail of SAR imagery. The despeckle filter demonstrates several distinctive characteristics when compared with some of the established filters: (1) it uses local statistics rather than global

statistics to determine speckle noise; (2) it replaces only the speckle noise without changing valid values; (3) it uses the original local median rather than the derived mean value to substitute for the detected speckle noise; and (4) it uses only valid pixel values to obtain the local median rather than all of the values in a moving window. As a result, the proposed filter not only effectively reduces/removes speckle noise, but also preserves important image structure, such as edges, linear features, and fine details, even in low-contrast areas.

Speckle Suppression Techniques

Two categories of techniques have been employed to suppress or remove speckle noise. The first category involves techniques such as multiple-look processing, which averages together several independent images or "looks" of different portions of the available azimuth spectral bandwidth (synthetic aperture), or different polarization states of the same area during image formation (Lee et al., 1994; Lillesand et. al., 2004). For example, one of the datasets used in this research was acquired with JERS-1 SAR systems, which has multi-look capability and thus the dataset was pre-processed using this technique. However, the other dataset used was acquired by the RADARSAT SAR in Fine Beam Mode, which is a single-look and did not undergo such a process, and appears to be more speckled. The second category includes techniques that smooth the image using digital image processing after the image is formed. There are two major approaches to speckle reduction using digital image processing. The first approach to digital filtering is achieved in the frequency domain, including the use of a Wiener filter (Walkup and Choens, 1974) or wavelet transformation (Gagnon and Jouan, 1997; Dong et al., 1998; Fukuda and Hirosawa, 1998; Simard et al., 1998). The second approach is accomplished in the spatial domain, where noise is removed by averaging or statistically manipulating the values of neighboring pixels. A good comparison of frequency domain (wavelet)–based and spatial domain (statistics)–based filters is provided by Hervet et al. (1998). The research described in this paper focuses on the second approach, specifically the employment of digital filters in the spatial domain to reduce the speckle in SAR imagery. In this way, the proposed filter can be compared with other statistics-based digital filters commonly available in commercial remote sensing software packages such as Leica GeoSystems ERDAS Imagine and Research Systems ENVI.

Most of these popular digital filters have been reviewed by Lee et al. (1994) and Sheng and Xia (1996). Two of the simplest despeckle filters are the mean (box) filter and median filter, in which the central pixel of a moving window is replaced by its mean and median, respectively. Following the assumption of the multiplicative noise model of the speckle effect, many other adaptive filters or algorithms have also been devised, including the Lee filter (Lee, 1980, 1981), Frost filter (Frost et al., 1981, 1982), Kuan filter (Kuan et al., 1985), Gamma (MAP or Maximum *A Posteriori*) filter (Kuan et al., 1987; Lopes et al., 1993), and Lee-sigma filter (Lee, 1983). All of these adaptive filters aim to effectively reduce speckle in radar images without eliminating the fine details (Jensen, 2004).

The mean filter is one of the most widely used low-pass filters (LPF). It does an excellent job of smoothing areas, but creates problems in that it smears the edges and fine features together with the speckle noise, thus failing to preserve image structure.

The median filter is successful at removing pulse and spike noise while retaining step and ramp functions (ERDAS Inc., 1999); therefore, the median filter is better than the mean filter in terms of preserving the edges between two different features, but it does not preserve single pixel-wide features, which will be altered if speckle noise is present (Smith, 1996). Lee et al. (1994) found that the 3×3 median filter preserves the texture information very well but does not retain the mean value at an acceptable level. The mean and median filters meet with only limited success when applied to SAR data. One reason for this is the multiplicative nature of speckle noise, which relates the amount of noise to the signal intensity. The other reason is that they are not adaptive filters in the sense that they do not account for the particular speckle properties of the image.

Adaptive filters, such as the Lee filter, are based on the assumption that the mean and variance of the pixel of interest are equal to the local mean and variance of all pixels within the user-selected moving window (Lee, 1980, 1981). The Lee filter removes the noise by minimizing either the mean square error or the weighted least square estimation. The Frost filter replaces the pixels of interest with a weighted sum of the values within the moving window (Frost et al., 1981, 1982). The weighting factors decrease with distance from the pixel of interest and increase for the central pixels as variance within the window increases. This filter assumes multiplicative noise and stationary noise statistics. The Kuan filter first transforms the multiplicative noise model into a signal-dependent additive noise model (Kuan et al., 1985). Then, the minimum square error criterion is applied. The resulting filter has the same form as the Lee filter but with a different weighting function. The Gamma (MAP: Maximum A *Posteriori*) filter was developed by Lopes et al., (1993) based on the improved Kuan MAP filter (Kuan et al., 1987). *A priori* knowledge of the probability density function of the scene is required before the filter can be applied. The scene reflectivity is assumed to be a Gamma distribution instead of a Gaussian distribution and the filtering process is controlled by setting two thresholds. However, the Gamma (MAP) filter, like the Frost filter, will blur the edges.

The Lee-sigma filter is a conceptually simple but effective alternative to the Lee and other sophisticated adaptive filters (Lee, 1983). It is one of the most widely used despeckle filters for SAR imagery and is based on the sigma probability of the Gaussian distribution. It first computes the sigma (i.e., standard deviation) of the entire scene, and then replaces each central pixel in a moving window with the average of only those neighboring pixels that have an intensity value within a fixed sigma range of the central pixel. Lee et al. (1994) concluded that, as a simple modification of the commonly used low-pass filter, surprisingly, the Lee-sigma filter is at least as effective as the more elaborative adaptive filters listed above, but significantly more computationally efficient. Moreover, the Lee filter is reportedly superior in its ability to preserve prominent edges, linear features, point target, and texture information. However, due to the use of a fixed sigma computed for the entire scene, Eliason and McEwen (1990) found that the Lee sigma filter blurred some of the low-contrast edges and linear features. They suggested a refined version using the local standard deviation for each moving window as the sigma parameter. Unlike other adaptive filters for smoothing speckle noise, this filter is adaptive to local variance instead of the variance of the whole image, and is often referred to as the local sigma filter. The

local sigma filter is thought to improve the effectiveness of the Lee-sigma filter, while avoiding over-smoothing of the low-variance areas (Eliason and McEwen, 1990).

METHODOLOGY

Nezry et al. (1993) argued that an ideal speckle filter should incorporate the advantages of the median speckle filter in structure retention, the adaptability of the Lee or Frost filter to the local speckle and scene statistics, and the simplicity and effectiveness of the Lee-sigma filter for speckle reduction. In light of these comments, a local adaptive median filter was developed that has the goal of sufficiently reducing or removing speckle noise without sacrificing image structures such as edges, linear features, and fine details. The performance of this proposed filter is evaluated and compared with the aforementioned adaptive filters, which are commonly available in commercial image processing software, such as ERDAS Imagine and Research Systems ENVI. The comparison was made based on both qualitative and quantitative performance criteria, including a speckle suppression index, speckle image statistical analysis, feature preserving index, edge enhancing index, and image detail preserving index, as well as visual assessment. The filters were applied to two different kinds of real-world SAR datasets—a JERS-1 image and a RADARSAT image.

Local Adaptive Median Filter

Similar to the Lee-sigma filter, the proposed filter is also conceptually simple and involves the computation of only simple statistics, such as means, medians, and standard deviations. However, when determining the sigma value, the strategy used by the local sigma filter proposed by Eliason and McEwen (1990) was adopted. The local sigma (standard deviation) is computed for each moving window rather than using the fixed sigma for the entire scene. Together with the local mean and a user-determined multiplier (usually between 1 and 2), the local sigma then helps to determine the range of the valid pixel intensity in the moving window. The thresholds of the valid pixel range for the proposed filter are the values of the local mean (instead of the central pixel value as with the local sigma filter) plus and minus the specified multiple of the local sigma. Each pixel value in the moving window is then tested against this valid pixel value range. Pixels with value outside the range are labeled as speckle noise; otherwise, they are assumed to be valid pixels. The fundamental difference of the proposed filter from the Lee-sigma and local sigma filters is that the proposed filter only replaces a central pixel if it is identified as speckle noise. If the central pixel is labeled as a valid pixel, no replacement will occur and the central pixel will retain its original values. Furthermore, unlike another filter devised by Eliason and McEwen (1990) for bit error removal (i.e., the adaptive box filter), the proposed filter uses the local median value rather than the local mean value to replace the central speckle pixel value. The local median is computed from the pixels identified to contain valid values instead of all of the pixels in the moving window. The detailed algorithm for the local adaptive median filter is given as follows.

Assume $D(i, j)$ is a moving window centered at pixel $d(i, j)$ with a window size of $2k + 1$ (where k is an integer). In this case, the window size is equal in both

dimensions and has to be an odd number, such as 3, 5, 7, etc. To calculate the local mean and local standard deviation, it is necessary to first obtain the sum $S(i, j)$ of all the *N(i,j)* pixel values in the moving window.

$$S(i,j) = \sum_{m=i-k}^{i+k} \sum_{n=i-k}^{j+k} d(m,n)$$

$$N(i,j) = (2k+1)^2$$

The local mean $\mu(i, j)$ of the moving window D is then computed as

$$\mu(i,j) = \frac{S(i,j)}{N(i,j)},$$

and the local standard deviation $\sigma(i, j)$ is calculated as

$$\sigma(i,j) = \sqrt{\frac{\sum_{m=i-k}^{i+k} \sum_{n=i-k}^{i+k} (d(i,j) - \mu(i,j))^2}{N(i,j)}}.$$

The range of valid pixel values can thus be determined by the above local statistics and a user-defined multiplier M. The lower bound $LB(i, j)$ and upper bound $UB(i, j)$ are defined as

$$LB(i,j) = \mu(i,j) - M\sigma(i,j)$$
$$UB(i,j) = \mu(i,j) + M\sigma(i,j).$$

Valid pixels and speckle are then identified and labeled in a separate mask with moving window L centered at $l(i, j)$. For every pixel $l(m, n)$

$$l(m,n) = 0 \text{ if } d(m,n) < LB(i,j) \text{ or } d(m,n) > UB(i,j)$$
$$l(m,n) = 1 \text{ if } LB(i,j) \le d(m,n) \le UB(i,j),$$

where $i - k \le m, n \le i + k$, 0 indicates speckle noise, and 1 a valid pixel. It is important to note that a non-central pixel outside the range in the current moving window may not be a speckle in another moving window centered on it.

If the central pixel $l(i, j)$ at the mask moving window L equals 0 (i.e., labeled as speckle), then only the original central pixel value $d(i, j)$ is replaced by the local adaptive median $r(i, j)$ of the local window, which is the median of all the values of the pixels that are labeled as valid, excluding speckle pixels. The local adaptive median *r(i,j)* is calculated as

$$r(i,j) = \text{median } (d(m,n))$$

where $l(m, n) = 1$ and $i - k \le m, n \le i + k$.

Performance Evaluation Measures

To assess the capability of the proposed filter to remove speckle noise, and its effectiveness in successfully preserving the intrinsic structure of the scene backscatter, several quantitative performance measures suggested in the review by Lee et al. (1994) and by Sheng and Xia (1996) were used. Some measures provide evaluation for a filter's speckle suppression capability, some assess a filter's preservation of image detail and linear structures, and others estimate a filter's retention of the mean value of a distributed target. The results of these measures can be contradictory. For example, a filter yielding good results in speckle suppression may perform poorly in preserving image detail, and vice versa. The use of multiple criteria helps to assess a filter's performance on the basis of its ability to yield an optimum tradeoff among different objectives. In addition to these quantitative measures, qualitative visual inspection is also used to compare results from different filters.

Speckle Suppression Index (SSI)

One of the commonly used measurements for speckle strength is the coefficient of variance, or the ratio of the standard deviation to the mean (Lee et al., 1994). It remains constant over homogeneous areas, where it is fully determined by the amount of speckle in the image (Hagg and Sties, 1996). The *speckle suppression index* (SSI) is the coefficient of variance of the filtered image normalized by that of the original image, which is defined as:

$$SSI = \frac{\sqrt{Var(R_f)}}{Mean(R_f)} \cdot \frac{Mean(R_f)}{\sqrt{Var(R_f)}},$$

where R_f is the filtered image value and R is the original image value. Compared with the original image, a filtered image tends to have less variance because speckle is suppressed. Therefore SSI is generally less than 1.0, and the smaller the SSI value, the greater the speckle suppression (Sheng and Xia, 1996).

Speckle Image Statistical Analysis (SISA)

Radar image speckle is multiplicative in nature. Therefore, the ratio of the original image and the filtered image is actually an image that represents the amplitude of the speckle:

$$SP = \frac{R}{R_f},$$

where SP is the resulting speckle image. Statistics, such as its mean and standard deviation, can be computed for this ratio or speckle image. Ideally, the histogram of the speckle image would have a normal distribution with a mean around 1.0. The mean of the speckle image is a good indicator of a filter's ability to retain an image's original mean values: the closer the mean is to 1.0, the better is the filter's ability in

retaining image content. The standard deviation of the speckle image, on the other hand, is also a measurement of the speckle suppression capability of the filter. In fact, it is inversely related to SSI described above (Sheng and Xia, 1996) and therefore was not used in this study.

Edge-Enhancing Index (EEI)

The edge-enhancing index is an important parameter in assessing the enhancement of step functions in an image. It is often used to evaluate a filter's ability to preserve edges, such as boundaries between water bodies and land. The EEI is defined as

$$EEI = \frac{\sum |R_{f1} - R_{f2}|}{\sum |R_1 - R_2|},$$

where, R_1 *and* R_2 are the original values of the pixels on either side of the edge, whereas R_{f1} and R_{f2} are the corresponding filtered values. The numerator is the absolute difference in intensity of the pixels on the two sides of the edge in the filtered image and the denominator is that difference in the original image. Therefore, the EEI is usually smaller than 1.0, and higher EEI values correspond to a better edge preserving capability.

Feature-Preserving Index (FPI)

The feature-preserving index is a measure for assessing a filter's ability to preserve linear features and subtle structure. For a one-pixel wide linear feature of n-pixel length, the FPI is given by

$$FPI = \frac{\sum_{1}^{n} (2 \cdot R_f - R_{f1} - R_{f2})}{\sum_{1}^{n} (2 \cdot R - R_1 - R_2)},$$

where R is the original value of a pixel on the linear feature, $R1$ and $R2$ are the neighboring pixels on both side of the feature, and R_f, R_{f1}, and R_{f2} are the filtered values of the corresponding pixels. In most cases, the values of a FPI measure are also lower than 1.0. The higher the FPI measure, the better the linear feature being preserved.

Image Detail–Preserving Coefficient (IDPC)

The image detail–preserving coefficient (IDPC) is the correlation coefficient between the original image and the filtered image. This correlation coefficient serves as an indicator of a filter's ability to preserve the fine details and subtle structures,

such as point features. The higher the IDPC, the better is the detail preservation capability of the filter.

Visual Comparison

Although quantitative measures are often employed to compare different speckle suppression filters, it has been noted by Raouf and Lichtenegger (1997) and others that visual inspection probably provides the best assessment of the performance of the speckle filter. Visual assessment is an easy and efficient way to investigate both a filter's capability to suppress speckle and its effectiveness in preserving image details.

A meaningful measure for the preservation of texture by the speckle filter is difficult to establish because fine texture is close to the speckle noise level. Therefore, the evaluation of texture preservation is subjective and is not included in this study. Lee et al. (1994) stated that, in general, filters using small windows (such as 3 × 3) preserve texture information better.

The SAR Datasets

Two different kinds of SAR datasets, JERS-1 and RADARSAT, depicting the same area in the Tivoli North Bay (N42°02', W73°55') of New York were used to assess the performance of the proposed despeckle filter. The JERS-1 SAR data were acquired on the July 3, 1993 and the RADARSAT SAR data were acquired on August 10, 1998. The JERS-1 SAR is an L-band system (23.5 cm wavelength) with HH polarization, 38.5° incidence angle, and 18 nominal resolution, while the RADARSAT SAR is a C-band system (5.6 cm wavelength) with HH polarization. RADARSAT's Fine Beam Mode offers a 37.99° incidence angle and 10 m resolution. Figure 1 displays the two raw images and the selected homogeneous areas, edges, and linear features to be used to compute some of the aforementioned performance measures.

RESULTS AND DISCUSSION

To evaluate the proposed filter's capability in minimizing speckle effects while preserving image content and detail, a number of established filters were applied to both the RADARSAT and JERS-1 data, including the Lee filter, Frost filter, Kuan filter, Gamma (MAP) filter, the local-sigma filter, and the Lee-sigma filter. Research Systems' ENVI 3.6 implementation of these filters was employed, except for the Lee-sigma filter, which was applied using ERDAS Imagine 8.6 software. The proposed filter was implemented in an ArcGIS application development environment using map algebra functions. All of the filters available in ENVI were applied using default system parameters, whereas the Lee-sigma filter and the proposed filter were applied with a user-defined multiplier value of 1.5. Various window sizes and multiple numbers of iterations of each filter were often tested in order to compare performance of the filters. All of the filters were applied with up to six iterations and with 3 × 3, 5 × 5, and 7 × 7 window sizes in order to fully understand the effects imposed by various window sizes and different number of iterations of each filter.

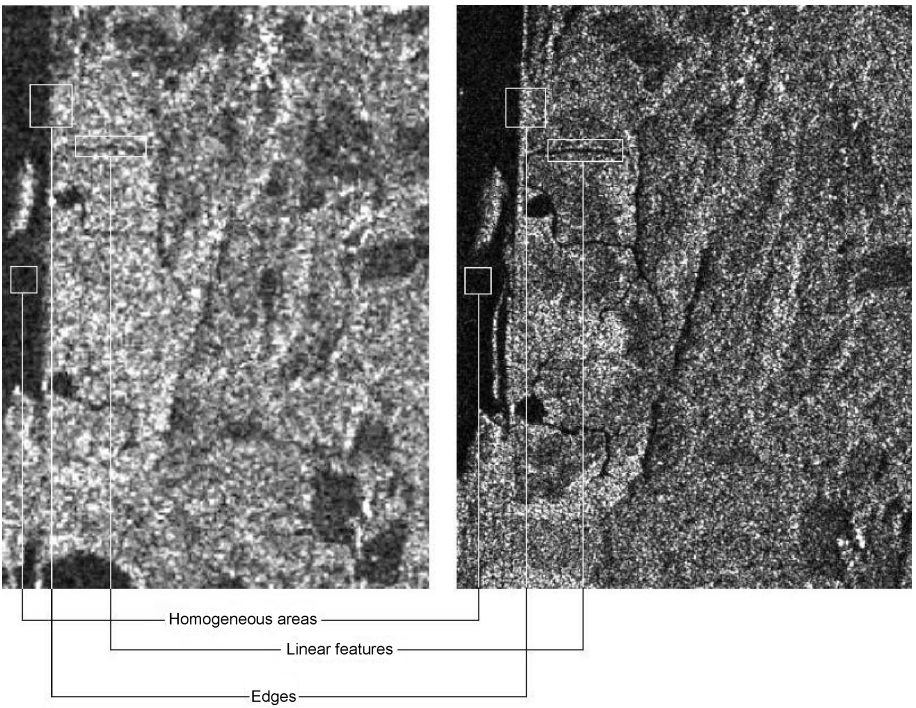

Fig. 1. Raw JERS-1 image (left) and RADARSAT image (right), with selected homogeneous areas, linear features, and edges.

Quantitative Assessment

Five of the aforementioned quantitative performance measures, including the speckle suppression index (SSI), speckle image statistical analysis (SISA), edge-enhancing index (EEI), feature-preserving index (FPI), and image detail–preserving coefficient (IDPC) index, were computed for each filtered image. The SSI values for the filtered JERS-1 and RADARSAT images derived from different filters with various window sizes and iterations are presented in Figures 2 and 3, respectively. Notice that by increasing the window size and the number of iterations, the SSI values was generally reduced (i.e., improved speckle suppression). However, such a trend is more obvious in the RADARSART data than the JERS-1 data, probably because the JERS-1 image has undergone multiple-look processing, which reduced much of the noise. With regards to the JERS-1 image (Fig. 2), the Lee-sigma filter outperformed all others and achieved the lowest SSI, providing best speckle suppression. The proposed filter exhibited slightly higher SSI values, but these values were very close in magnitude to the SSI values for most other filters. One thing worth noticing is that the performance of the proposed filter improves steadily with increasing window size and number of iterations. During the sixth iteration of the 7×7 moving window, the proposed filter outperformed all other filters except the Lee-sigma filter. As for the RADARSAT image (Fig. 3), the Gamma (MAP) filter achieved the best speckle suppression effect in all configurations. The proposed filter, along with the local sigma

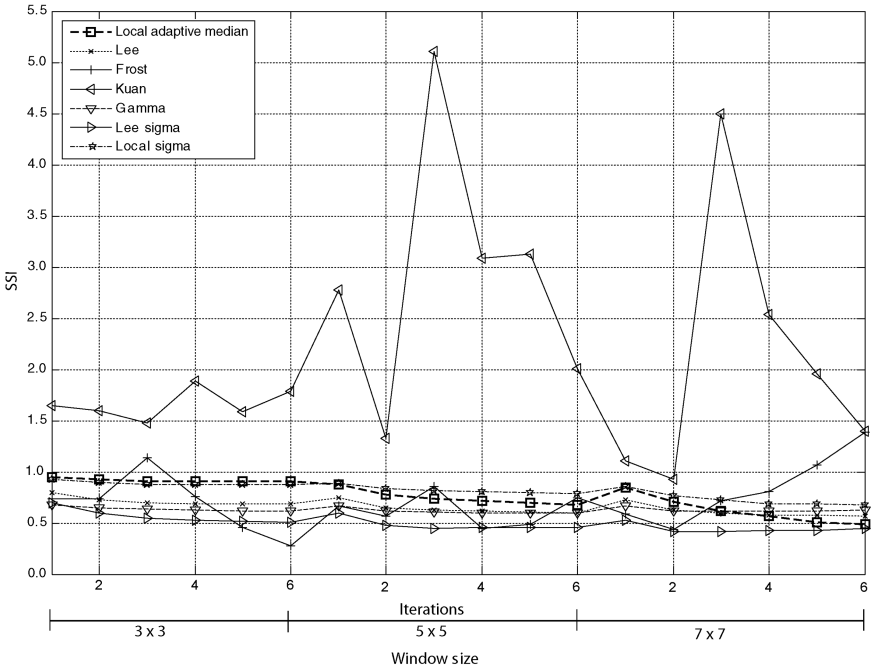

Fig. 2. Speckle suppression index (SSI) plot for the JERS-1 data.

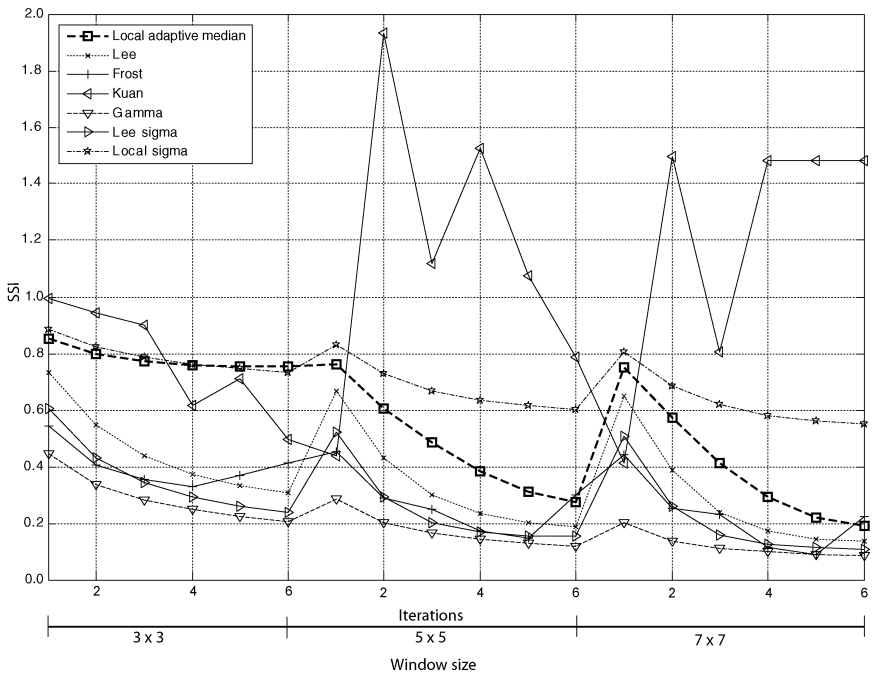

Fig. 3. Speckle suppression index (SSI) plot for the RADARSAT data.

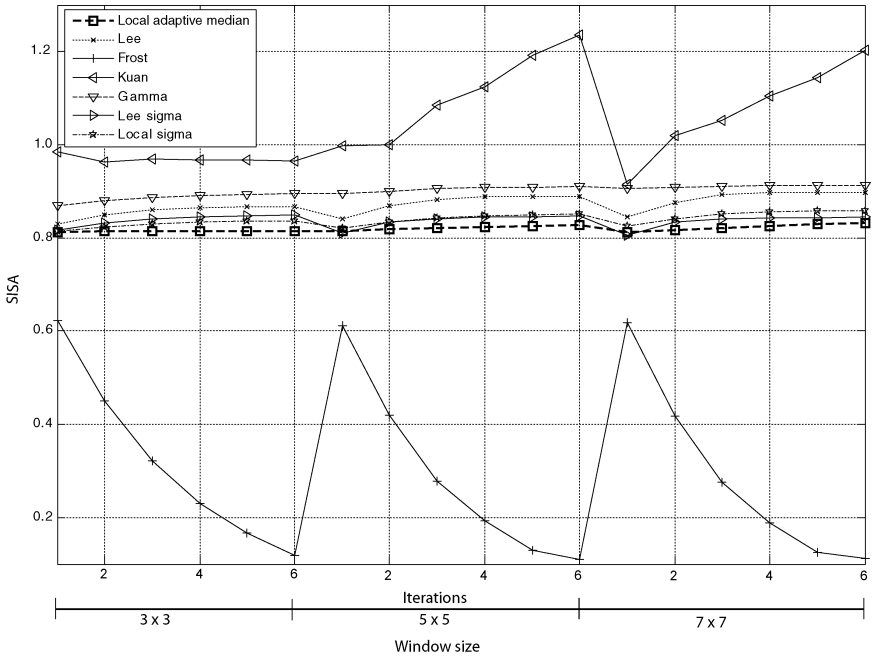

Fig. 4. Speckle image statistical analysis (SISA) mean plot for the JERS-1 data.

filter, attained moderate SSI values when a small window size (i.e., 3 × 3) was used. When larger window sizes were applied, the speckle suppression power of the proposed filter, unlike that of the local sigma filter, drastically improved as the number of iterations increased. Almost all of the filters reduced speckle to some extent as indicated by SSI values below 1.0. The Kuan filter, however, was an exception, exhibiting poor and unstable performance. In some cases, the application of the Kuan filter even introduced more speckle in the images, resulting in SSI values greater than 1.0.

The results of the speckle image statistical analysis (SISA) are displayed in Figures 4 and 5. Since the implication of the standard deviation parameter of the speckle image is similar to that of the SSI, only the mean values were compared. A well-performing filter should generate a speckle image that has a mean around 1.0, suggesting the majority of the pixel values in the original image are retained in the filtered image and much of the image content is preserved. The SISA measures for the JERS-1 and RADARSAT images gave a mixed picture. For the JERS-1 image (Fig. 4), most of the filters produced a speckle image with a mean that was less than 1.0, indicating an increase in intensity when compared with the original pixel values. The Kuan filter yielded mean values that were closest to 1.0 when the window size was small, but its mean values increased rapidly when larger window sizes were used, especially with an increasing number of iterations. The speckle images derived using the proposed filter, along with the Lee, Gamma (MAP), local sigma, and Lee-sigma filters, yielded steady mean values between 0.8 and 0.9, indicating that their ability to retain the original pixel intensity does not change with window size or from iteration to iteration. The Frost filter resulted in speckle images with means in a range from

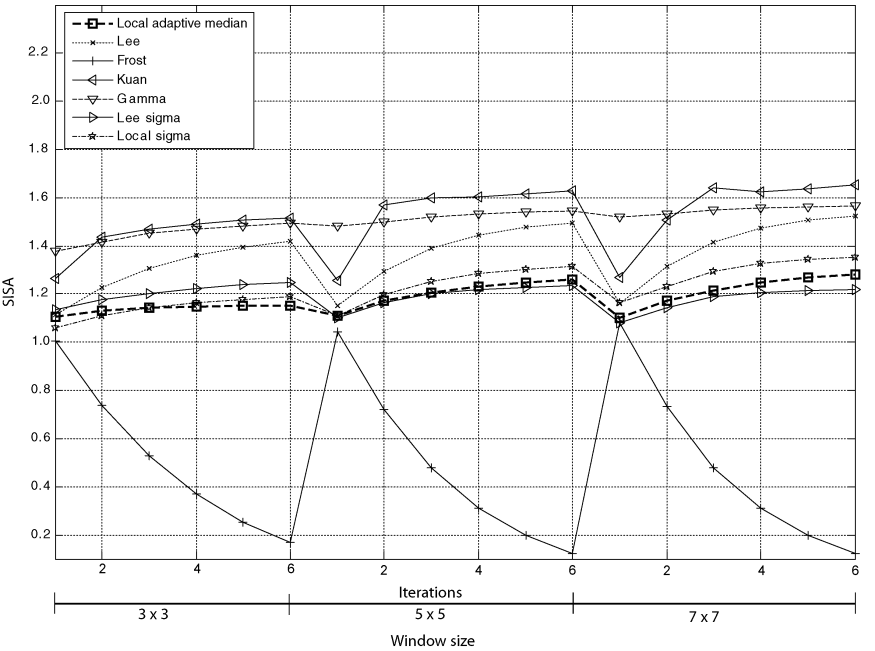

Fig. 5. Speckle image statistical analysis (SISA) mean plot for the RADARSAT data.

0.5 to 0.2, suggesting poor performance in keeping the original pixel values. For RADARSAT data (Fig. 5), however, most of the filters resulted in a speckle image with means greater than 1.0, signifying a possible reduction of intensity when compared to the original pixel values. The proposed filter, together with the Lee-sigma and local sigma filters, surpassed other filters with means for speckle around 1.2. The means of the Kuan and Frost filters were unacceptably high and low, respectively.

The edge-enhancing index (EEI) that is used to represent the edge preserving capability of the filter is presented in Figures 6 and 7. In the case of JERS-1 data (Fig. 6), the proposed filter exhibited the best overall edge-preserving performance, especially with the 3 × 3 moving window. Except for the local sigma filter that could occasionally compete with the proposed filter, most of the other filters produced relatively low EEI values in general, especially after the first iteration. The EEI values for the Kuan filter again varied widely, with an abnormally high value at the second iteration of the 7 × 7 moving window. For the RADARSAT image, (Fig. 7), the proposed filter consistently outperformed other filters in almost all cases. When the 3 × 3 moving window was used, the proposed filter yielded perfect edge-preserving results with all of the EEI values equal to 1. The local sigma and Lee filters displayed a modest edge-preserving capability (with EEI values generally > 0.5), while the performance of the rest of the filters, including the Kuan, Gamma (MAP), Lee-sigma and Frost filters, was less than promising and practically unacceptable.

The ability of various filters to retain linear features as evaluated by the feature preserving index (FPI) is displayed in Figures 8 and 9. The FPI values derived from the JERS-1 image are generally lower than those obtained from the RADARSAT

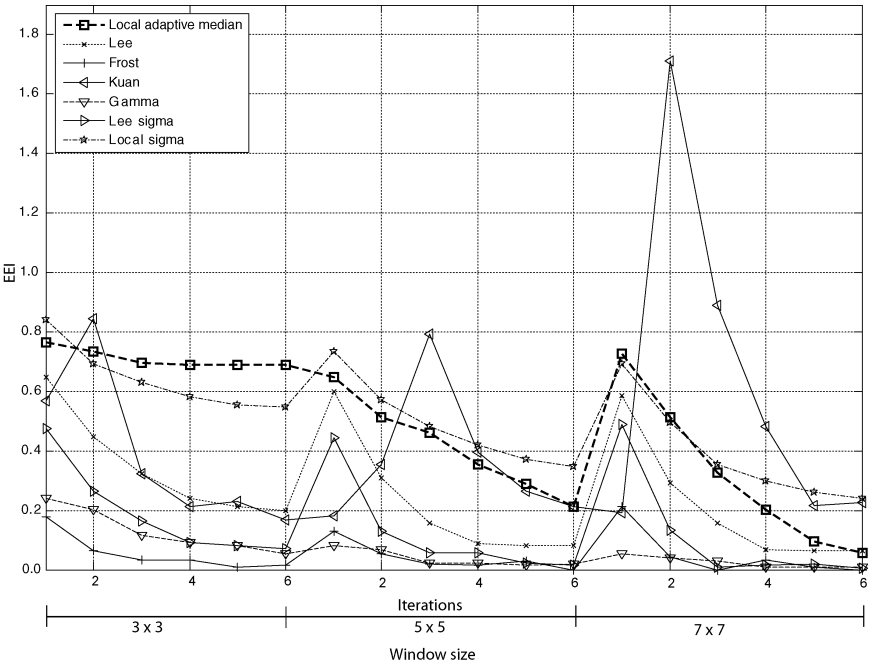

Fig. 6. Edge-enhancing index (EEI) plot for the JERS-1 data.

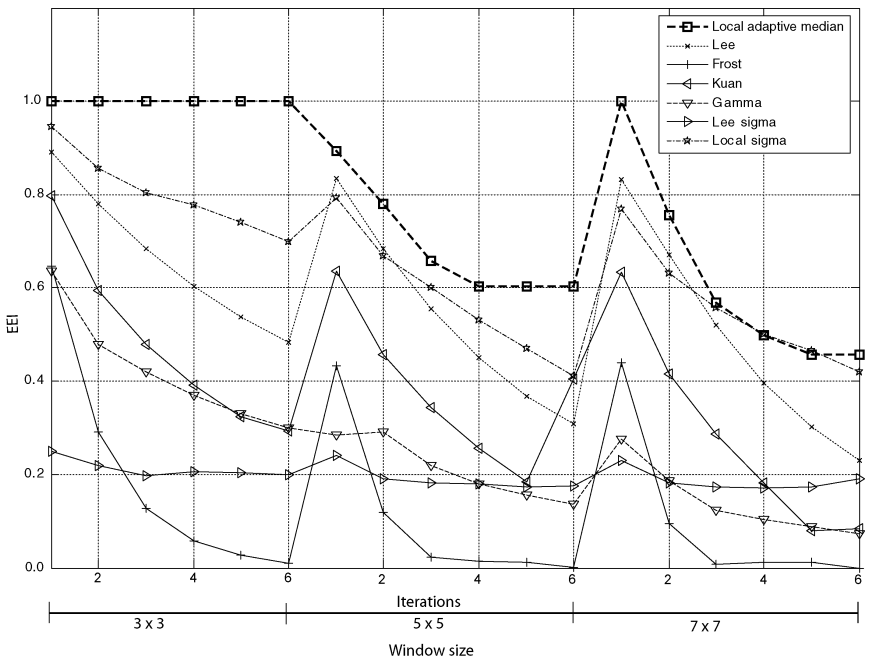

Fig. 7. Edge-enhancing index (EEI) plot for RADARSAT data.

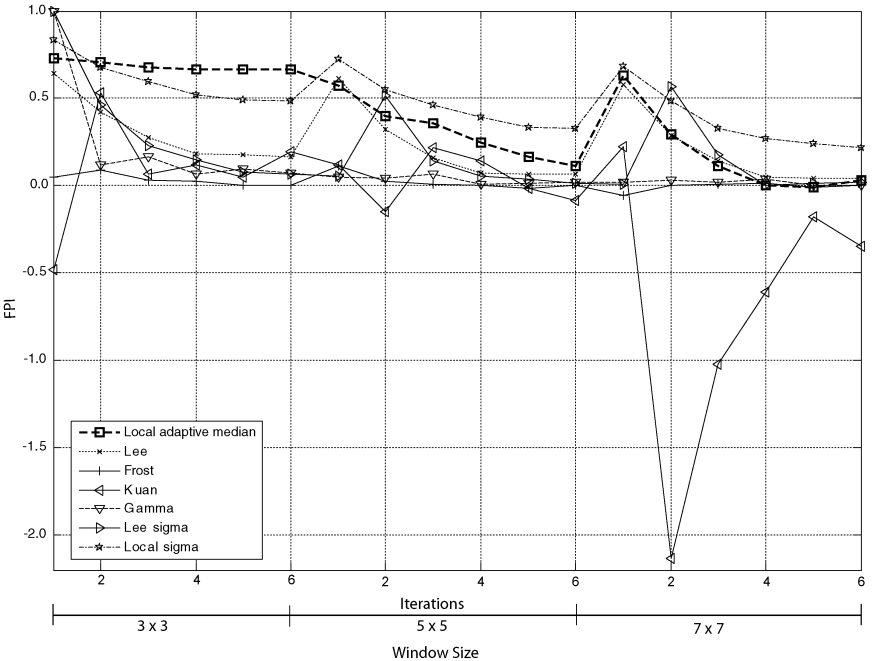

Fig. 8. Feature-preserving index (FPI) plot for the JERS-1 data.

image for the same reason mentioned above. For the JERS-1 image (Fig. 8), the proposed filter appears to be the best feature preserver for all iterations when a small 3 × 3 window is used. When larger window sizes were used, the local sigma filter resulted in slightly higher FPI values than the other filters. Regarding the RADARSAT image (Fig. 9), especially high FPI values (almost 1.0) were observed for the proposed filter and Lee-sigma filter alike, when a small 3 × 3 moving window was applied. The proposed filter yielded consistently higher FPI values than the other filters, although, like most of the other filters, the FPI values decreased with increasing numbers of iterations and larger window sizes. The Kuan filter again demonstrated an unpredictable pattern of FPI values, which was also observed in the results of the JERS-1 image.

The image detail–preserving coefficient (IDPC) index is the correlation coefficient between the original and the filtered images. For the JERS-1 image (Fig. 10), the local sigma filter outperformed all of the other filters. The proposed filter, as well as the Lee and Gamma (MAP) filters, all demonstrated strong IDPC values (between 0.8 and 1.0), while the Frost and Kuan filters tended to have low IDPC values. For the RADARSAT image (Fig. 11), the IDPC values of most filters were slightly lower when compared to those of the JERS-1 image. However, the majority of the filters still have IDPC values generally > 0.5 except for the Frost filter. The proposed filter achieved steady and high IDPC values > 0.8 for all of the iterations of the 3 × 3 moving window and for the first two iterations of the 5 × 5 windows. When larger window sizes were applied, most filters yielded a steady decrease in the IDPC values.

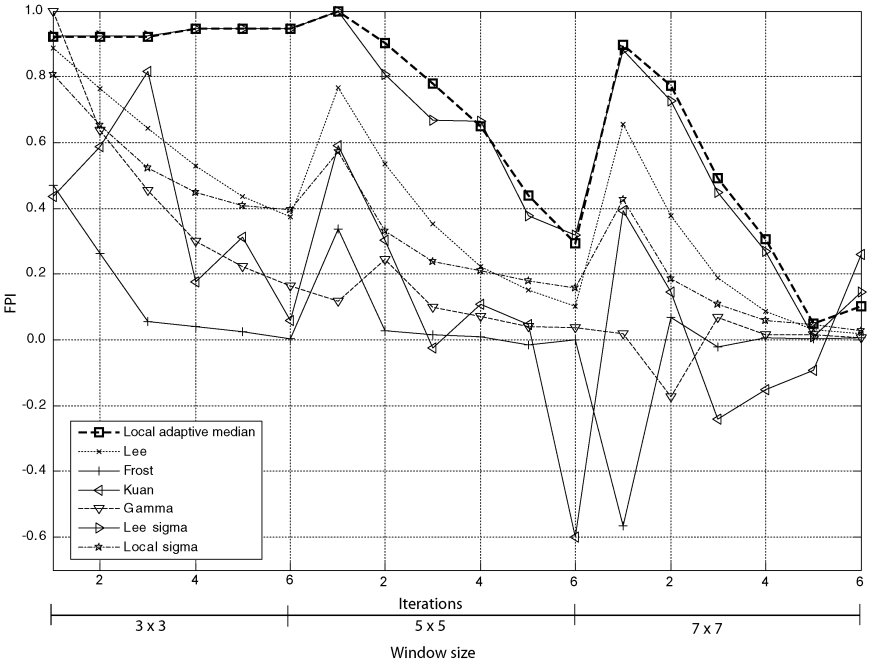

Fig. 9. Feature-preserving index (FPI) plot for the RADARSAT data.

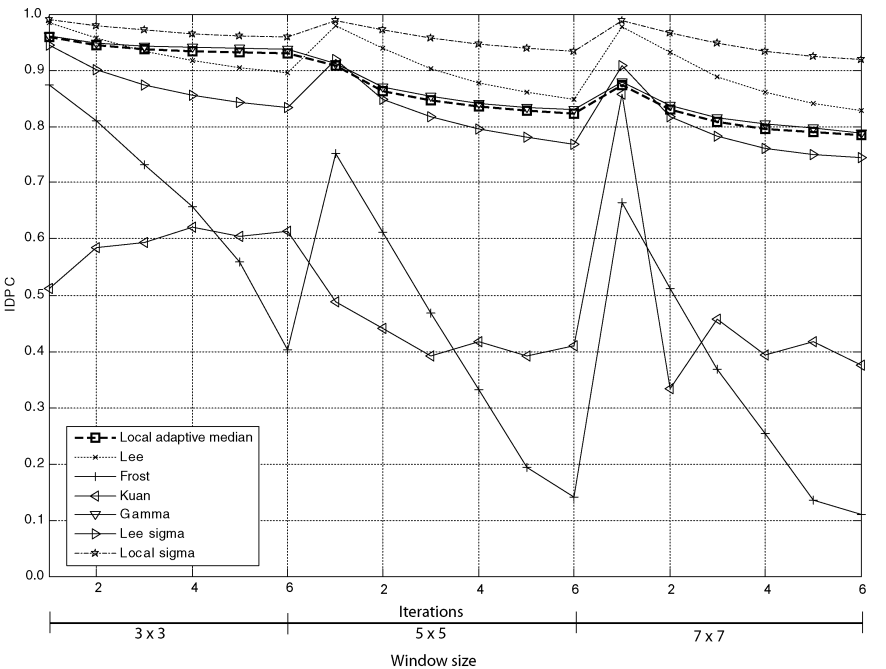

Fig. 10. Image detail–preserving coefficient (IDPC) plot for the JERS-1 data.

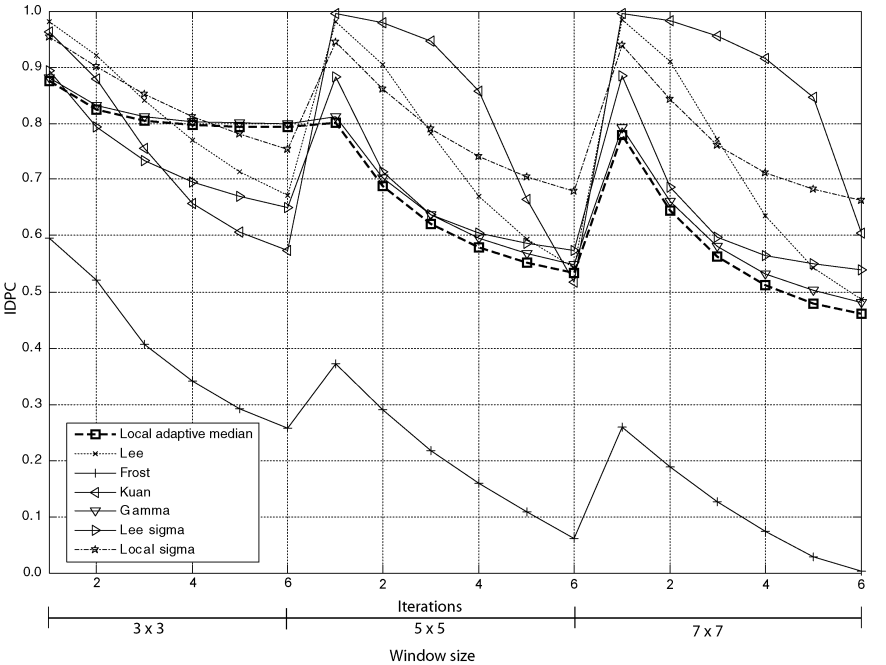

Fig. 11. Image detail–preserving coefficient (IDPC) plot for the RADARSAT data.

As demonstrated by these quantitative measures of performance, the proposed filter yielded the highest SISA, EEI, FPI, and IDPC values when applied to the RADARSAT data in almost all of the cases, but at the cost of a slightly lower SSI value. This indicates that the proposed filter was especially effective in preserving the original data content, boundary edges, linear features, and fine details of an extremely speckled image single-look RADARSAT image. Except when a small moving window was used, the proposed filter achieved speckle suppression effects that were superior to the local sigma and Kuan filters, and comparable to most other established filters, including the Lee, Frost, Gamma (MAP), and Lee-sigma filters. When applying filters to less speckled SAR data that has been preprocessed using the multiple-look averaging approach, such as the JERS-1 data, the proposed filter achieved a better SSI than that for the RADARSAT image. Although the SISA, EEI, FPI, and IDPC values obtained for the JERS-1 data were not always the best, the performance of the proposed filter in retaining image content, edges, linear features, and fine details was often superior or at least equivalent to other established filters. Therefore, the proposed filter appears to have achieved a good balance between speckle reduction and structure retention based on a comparison of the quantitative performance measures.

Visual Assessment

In order to visually assess the performance of the filters in a close-up view, subsets of the study area that contain homogeneous regions of a water body, edges

between water and land, linear features such as tidal channels, and other geographic details, were cropped from both the original and the filtered images of the JERS-1 and RADARSAT data (Figs. 12 and 13). For the JERS-1 data, the images resulting from the third iteration of the filters using a 3 × 3 moving window were selected and displayed for the purpose of visual comparison (Fig. 12). For the RADARSAT data, the images at the fifth iteration using the a 3 × 3 moving window of the filters were chosen, because the single-look raw image contained more speckle noise and thus demanded more iterations of filtering (Fig. 13).

For the JERS-1 data (Fig. 12), the proposed filter demonstrated the best image detail–preserving ability along with the local sigma filter, and concurrently attained a sufficient speckle suppression effect. The local sigma filter, however, failed to eliminate dark speckles and produced a "splotchy" filtered image. The Lee filter substantially suppressed the speckle noise, but accomplished only a mediocre preservation of fine details, which resulted in many unnatural white regions in the image. The Frost, Kuan, Gamma (MAP), and Lee-sigma filers oversmoothed the original image and blurred the fine detail in the image. The Kuan filter, in particular, introduced many artifacts in the form of white squares, some with black boundaries.

For the RADARSAT data (Fig. 13), a similar pattern is observed as with the JERS-1 data. The Frost, Kuan, Gamma (MAP), and Lee-sigma filters obscured the linear features and other fine details, resulting in very "fuzzy" filtered images. The Lee filter, while considerably smoothing much of the speckle noise, also blurred many of the fine details and parts of the linear features present in the original image. The local sigma filter preserved the image details well, but inadequately reduced the speckle; much of the noise, both in black and white, is still quite apparent in the resulting image. The proposed filter not only achieved a detail-preserving effect comparable with that of the local sigma filter, but also effectively reduced the speckle noise, as evidenced by the homogenous regions of the water surface, although the resulting image is not as visually smooth as the Lee sigma filtered image. Based on this qualitative visual inspection, the proposed filter is considered to have best accommodated the tradeoff between speckle suppression and detail preservation among all filters. This agrees with what was observed using the quantitative measures of performance.

The Strength of the Proposed Filter

Both quantitative and visual assessments suggest that the proposed filter has considerable value. This success of the filter is attributed to the following filter characteristics. The use of the local standard deviation of the moving window helps to improve the differentiation of speckle noise from valid pixels by incorporating the local instead of global data distribution. Using the local mean instead of the central pixel value of a moving window to define the valid pixel range is more reasonable and adheres to the multiplicative nature of speckle noise. A potential problem associated with the use of the central pixel value to define the range arises if the central pixel itself is speckle noise; then other speckle with similar intensity in the moving window will not be easily detected. After the speckle noise is identified as being outside the valid pixel value range, the filter updates only the pixels that are labeled as being speckle noise, while valid central pixels are allowed to keep their original value. This

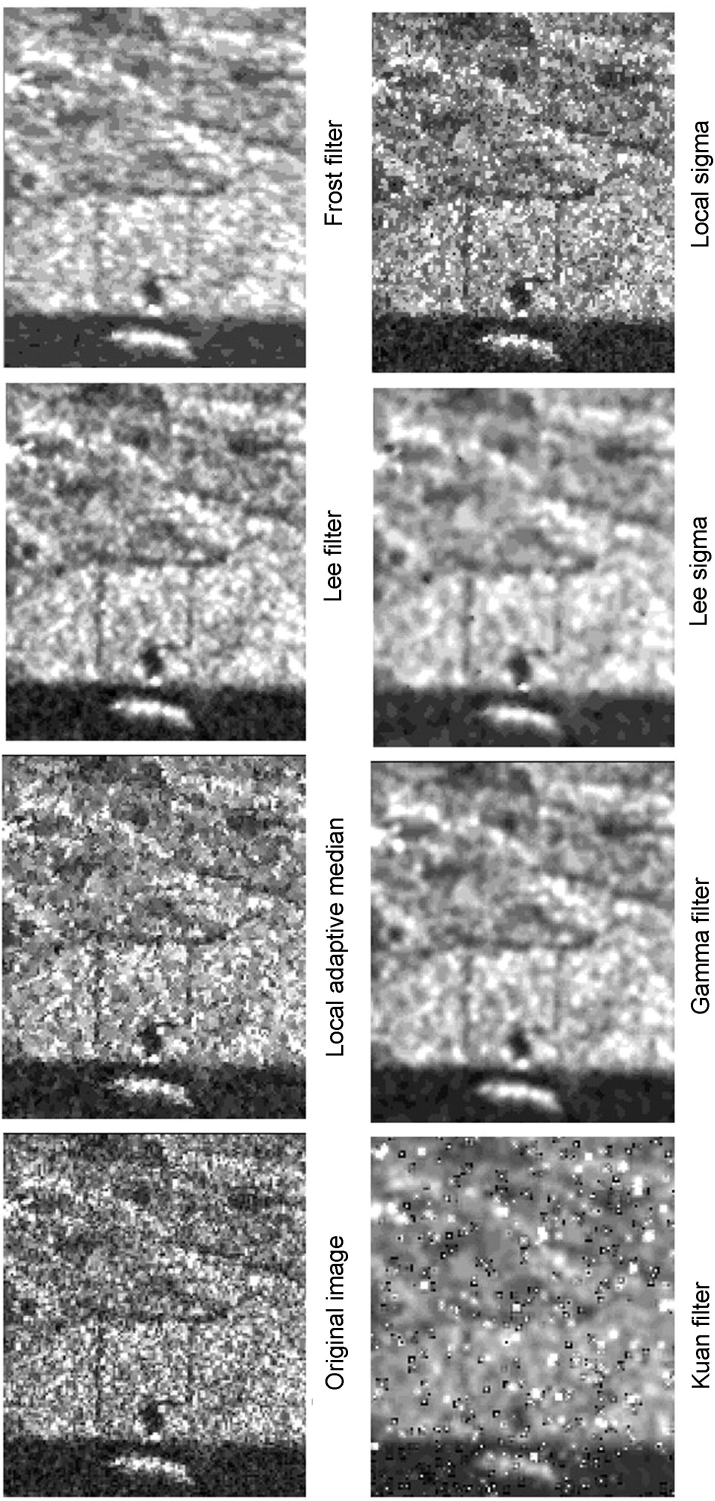

Fig. 12. Original and the filtered JERS-1 images resulting from the application of various filters at the third iteration of the 3×3 moving window.

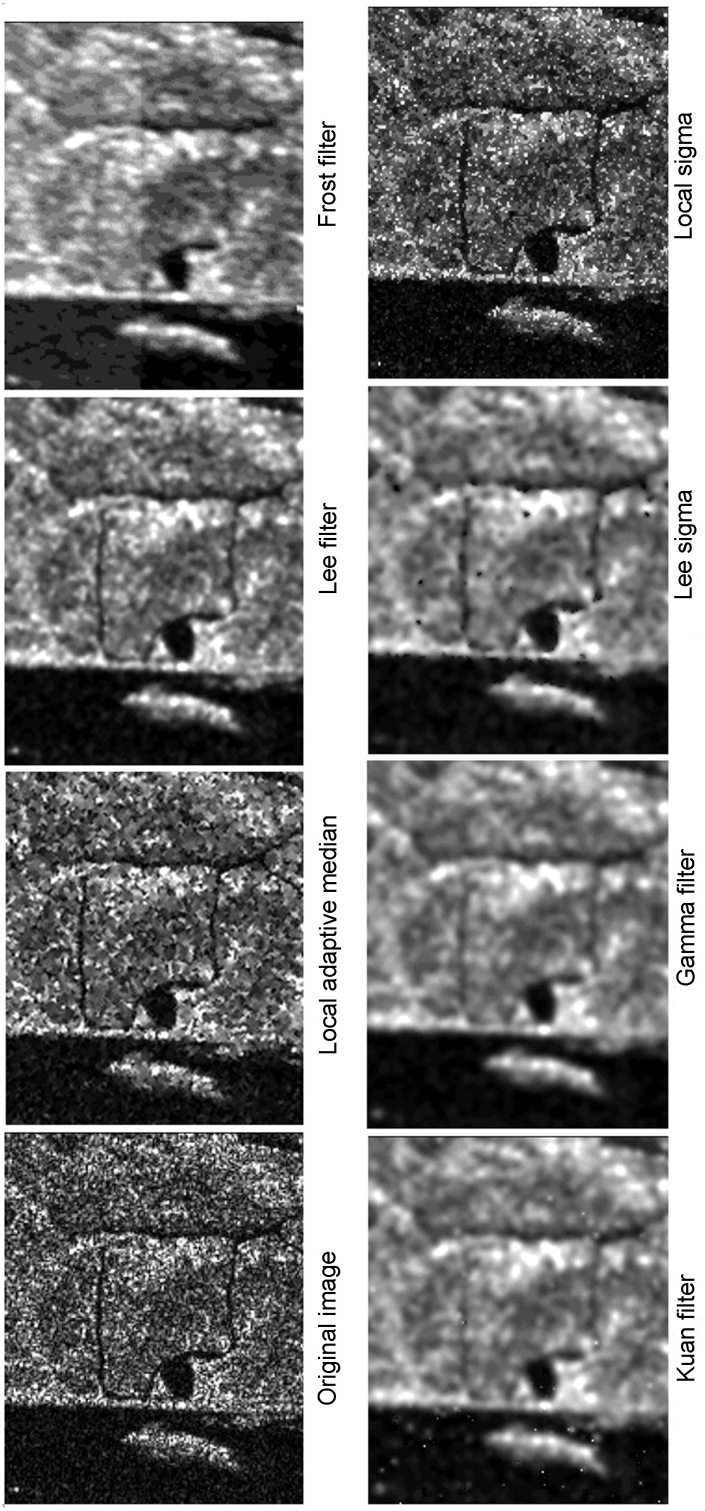

Fig. 13. Original and the filtered RADARSAT images resulting from the application of various filters at the fifth iteration of a 3×3 moving window.

helps to maintain the mean of the filtered image, and thus the original image content. Applying the median function only to the valid pixel values retains image details and preserves the linear features and edges better than that of the mean function in the local area. In a SAR image, low-valued and high-valued pixels often correspond to destructive and constructive speckle. The replacement of noise with the local median value helps to exclude the erroneous variations from the filtered image. Unlike replacing the speckle noise with the mean value, the employment of the local median value replaces the speckle with one of the original valid pixel values, instead of a derived value, which might have incorporated other speckle noise during the computation of the average.

CONCLUSION

The presence of speckle noise as grainy salt-and-pepper patterns in a SAR image often obscures the underlying image content, reduces the interpretability of the image, and complicates digital image processing. To take full advantage of active SAR data, the reduction of speckle is often desired. Substantially reducing speckle noise while effectively preserving image detail are two important speckle suppression considerations. In many applications, it is the balance between these two considerations that determines the success of a speckle suppression filter. For this reason, a new local adaptive median filter for speckle suppression was proposed. It attempted to integrate the advantages of the median filter in structure retention, the adaptability of the Lee or Frost filter to the local speckle and scene statistics, and the simplicity and effectiveness of the Lee-sigma filter for speckle reduction. The proposed filter computes the statistics of a moving window and determines speckle noise based on local mean and standard deviation information. An adaptive local median function is then used to replace the central speckle noise, while valid pixels keep their original values.

The performance of the proposed filter was evaluated using a number of quantitative and qualitative criteria. These included the speckle suppression index (SSI), speckle image statistical analysis (SISA), edge-enhancing index (EEI), feature-preserving index (FPI), and image detail–preserving coefficient (IDPC), in addition to visual assessment. Two different kinds of SAR datasets, RADARSAT Fine Beam Mode SAR and JERS-1 SAR data, were used for evaluation purposes. In comparison to many established adaptive filters, including the Lee filter, Frost filter, Kuan filter, Gamma (MAP) filter, the local sigma filter, and the Lee-sigma filter, it was found that the proposed filter not only achieved comparable effectiveness in speckle noise reduction, but also demonstrated superior capability in structure and detail preservation. In conclusion, the proposed filter is considered to be the best filter to accommodate the tradeoff between sufficient speckle suppression and effective detail retention among those evaluated in this study.

ACKNOWLEDGMENTS

The authors appreciate Dr. Ronald Briggs and Ms. Annie Hsu and other anonymous reviewers for reviewing the manuscript.

REFERENCES

April, G. V. and E. R. Harvy, 1991, "Speckle Statistics in Four-Look Synthetic Aperture Radar Imagery," *Optical Engineering*, 30(4):375-381.

Bruniquel, J. and A. Lopes, 1997, "Multivariate Optimal Speckle Reduction in SAR Imagery," *International Journal of Remote Sensing*, 18(3):603-627.

Dong, Y., Forester, B. C., Miline, A. K., and G. A. Moragan, 1998, "Speckle Suppression Using Recursive Wavelet Transforms," *International Journal of Remote Sensing*, 19(2):317-330.

Eliason, E. M. and A. S. McEwen, 1990, "Adaptive Box Filters for Removal of Random Noise from Digital Images," *Photogrammetric Engineering & Remote Sensing*, 56(4):453-458.

ERDAS Inc., 1999, *The Erdas Field Guide*, Atlanta, GA: ERDAS Press, 672 p.

Frost, V. S., Stiles, J. A., Shanmugan, K. S., and J. C. Holtzman, 1982, "A Model for Radar Images and Its Application to Adaptive Digital Filtering of Multiplicative Noise," *IEEE Transactions on Pattern Analysis and Machine Intelligence*, 4(2):157-166.

Frost, V. S., Stiles, J. A., Shanmugan, K. S., Holtzman, J. C., and S. A. Smith, 1981, "An Adaptive Filter for Smoothing Noisy Radar Images," in Proceedings of the IEEE, January 1981, 133-155.

Fukuda, S. and H. Hirosawa, 1998, "Suppression of Speckle in Synthetic Aperture Radar Images Using Wavelets," *International Journal of Remote Sensing*, 19(3):507-519.

Gagnon, L. and A. Jouan, 1997, "Speckle Filtering of SAR Images—a Comparative Study between Complex-Wavelet-Based and Standard Filters," in Proceedings of SPIE Wavelet Applications in Signal And Image Processing V, San Diego, CA, 80-91.

Goodman, J. W., 1976, "Some Fundamental Properties of Speckle," *Journal of the Optical Society of America*, 66(11):1145-1150.

Hagg, W. and M. Sties, 1996, "The Epos Speckle Filter: A Comparison with Some Well-Known Speckle Reduction Techniques," in Proceedings of the XVIII ISPRS Congress, July 9-19, 1996, Vienna, Austria, 135-140.

Hervet, E., Fjørtfort, R., Marthon, P., and A. Lopes, 1998, "Comparison of Wavelet-Based and Statistical Speckle Filters," in SPIE: EUROPTO Conference on SAR Analysis, Modeling, and Techniques, Society of Photo-Optical Instrumentation Engineers, September 1998, Barcelona, Spain, 1-12.

Jensen, J. R., 2000, *Remote Sensing of the Environment: An Earth Resource Perspective*, Upper Saddle River, NJ: Prentice Hall, 544 p.

Jensen, J.R., 2004, *Introductory Digital Image Processing—a Remote Sensing Perspective*, Upper Saddle River, NJ: Prentice Hall, 3rd Ed., 526 p.

Kuan, D. T., Sawchuk, A. A., Strand, T. C., and P. Chavel, 1985, "Adaptive Noise Smoothing Filter for Image with Signal-Dependent Noise," *IEEE Transactions on Pattern Analysis and Machine Intelligence*, 7(2):165-177.

Kuan, D. T., Sawchuk, A. A., Strand, T. C., and P. Chavel, 1987, "Adaptive Restoration of Images with Speckle," *IEEE Transactions on Acoustics, Speech, and Signal Processing*, 35(3):373-383.

Lee, J.-S., 1980, "Digital Image Enhancement and Noise Filtering by Use of Local Statistics," *IEEE Transactions on Pattern Analysis and Machine Intelligence*, 2(2):165-168.

Lee, J.-S., 1981, "Speckle Analysis and Smoothing of Synthetic Aperture Radar Images," *Computer Graphics and Image Processing*, 17(1):24-32.

Lee, J.-S., 1983, "A Simple Speckle Smoothing Algorithm for Synthetic Aperture Radar Images," *IEEE Transactions on Systems, Man, and Cybernetics*, 13(1):85-89.

Lee, J.-S., 1986, "Speckle Suppression and Analysis for Synthetic Aperture Radar Images," *Optical Engineering*, 25(5):636-643.

Lee, J.-S., Jurkevich, I., Dewaele, P., Wambacq, P., and A. Oosterlinck, 1994, "Speckle Filtering of Synthetic Aperture Radar Images: A Review," *Remote Sensing Review*, 8:313-340.

Lillesand, T. M., Kiefer, R. W., and J.W. Chipman, 2004, *Remote Sensing and Image Interpretation*, New York, NY: John Wiley & Sons, 763 p.

Lopes, A., Nezry, E., Touzi, R., and H. Laur, 1993, "Structure Detection and Statistical Adaptive Speckle Filtering in SAR Images," *International Journal of Remote Sensing*, 14(9):1735-1758.

Nezry, E., Mougin, E., Lopes, A., Gastellu-Etchegorry, J. P., and Y. Laumonier, 1993, "Tropical Vegetation Mapping with Combined Visible and SAR Spaceborne Data," *International Journal of Remote Sensing*, 14(11):2165-2184.

North, H. C. and Q. X. Wu, 2001, "An Edge Preserving Filter for Imagery Corrupted with Multiplicative Noise," *Photogrammetric Engineering & Remote Sensing*, 67(1):57-64.

Raouf, A. and J. Lichtenegger, 1997, "Integrated Use of SAR and Optical Data for Coastal Zone Management," in ERS Satellite Radar Imagery: Proceedings of the Third ERS symposium, 18–21 March 1997, Florence, Italy, ESA SP-1204 (CD-ROM).

Schulze, M. A. and Q. X. Wu, 1995, "Noise Reduction in Synthetic Aperture Radar Imagery Using a Morphology-Based Nonlinear Filter," in Proceedings of DICTA 95, Digital Image Computing: Techniques and Applications, 6–8 December, 1995, Brisbane, Australia, 661-666.

Sheng, Y. and Z.-G. Xia, 1996, "A Comprehensive Evaluation of Filters for Radar Speckle Suppression," in Proceedings of the International Geoscience and Remote Sensing Symposium, 27–31 May, 1996, Lincoln, NE, 1559-1561.

Shi, Z. and K. B. Fung, 1994, "A Comparison of Digital Speckle Filters," in Proceedings of the International Geoscience and Remote Sensing Symposium, August 8–12, 1994, Pasadena, CA, 2129-2133.

Simard, M., Degrandi, G., Thomson, T. B., and G. B. Benie, 1998, "Analysis of Speckle Noise Contribution on Wavelet Decomposition of SAR Images," *IEEE Transactions on Geoscience and Remote Sensing*, 36(6):1953-1962.

Smith, D. M., 1996, "Speckle Reduction and Segmentation of Synthetic Aperture Radar Images," *International Journal of Remote Sensing*, 17(11):2043-2057.

Walkup, J. F. and R. C. Choens, 1974, "Image Processing in Signal Dependent Noise," *Optical Engineering*, 13:250-266.

Xiao, J., Li, J., and A. Moody, 2003, "A Detail-Preserving and Flexible Adaptive Filter for Speckle Suppression in SAR Imagery," *International Journal of Remote Sensing*, 24(12):2451-2465.